Article

Cell Reports

M-CSF from Cancer Cells Induces Fatty Acid Synthase and PPARβ/δ Activation in Tumor Myeloid Cells, Leading to Tumor Progression

Graphical Abstract

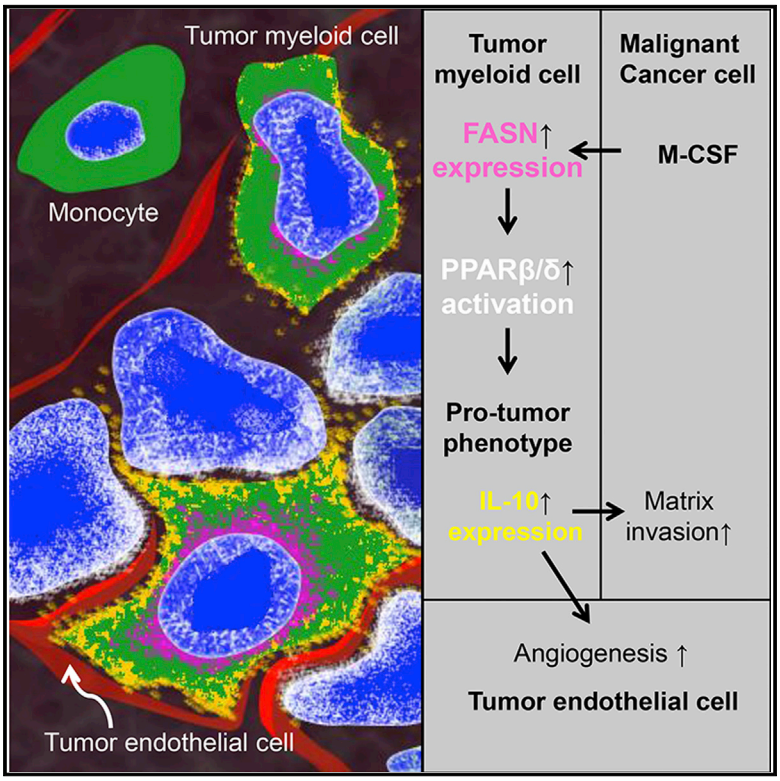

Highlights

- PPARβ/δ in tumor myeloid cells is critical to tumor progression and growth
- PPARβ/δ-dependent IL-10 expression promotes tumor angiogenesis and matrix invasion
- M-CSF from cancer cells stimulates PPARβ/δ activation of myeloid cell via FASN

Authors

Jonghanne Park, Sang Eun Lee, ..., Young Tae Kim, Hyo-Soo Kim

Correspondence

hyosoo@snu.ac.kr

In Brief

Park et al. show that PPARβ/δ in tumor myeloid cells enhances tumor angiogenesis and malignant cell invasion in an IL-10-dependent manner. This is initiated by M-CSF secreted from tumor cells, which activates PPARβ/δ in tumor myeloid cells via increased endogenous fatty acid synthase.

Park et al., 2015, Cell Reports *10*, 1614–1625
March 10, 2015
http://dx.doi.org/10.1016/j.celrep.2015.02.024

CellPress

OPEN ACCESS
CellPress

Cell Reports
Article

M-CSF from Cancer Cells Induces Fatty Acid Synthase and PPARβ/δ Activation in Tumor Myeloid Cells, Leading to Tumor Progression

Jonghanne Park,[1,2,3,8] Sang Eun Lee,[1,2,3,8] Jin Hur,[1,2,8] Eun Byeol Hong,[1,2] Jae-Il Choi,[1,2] Ji-Min Yang,[1,2] Ju-Young Kim,[1,2] Young-Chan Kim,[1,2] Hyun-Jai Cho,[1,2,3] Jeffrey M. Peters,[4] Seung-Bum Ryoo,[5] Young Tae Kim,[6] and Hyo-Soo Kim[1,2,3,7,*]

[1]National Research Laboratory for Cardiovascular Stem Cell Niche
[2]Innovative Research Institute for Cell Therapy
[3]Cardiovascular Center and Department of Internal Medicine
Seoul National University Hospital, Seoul 110-744, Korea
[4]Department of Veterinary and Biomedical Sciences and Center for Molecular Toxicology and Carcinogenesis, Pennsylvania State University, University Park, PA 16802, USA
[5]Department of Surgery, Seoul National University College of Medicine, Seoul 110-744, Korea
[6]Department of Thoracic and Cardiovascular Surgery, Biomedical Research Institute, Seoul National University Hospital, Seoul 110-744, Korea
[7]Molecular Medicine and Biopharmaceutical Sciences, Graduate School of Convergence Science Technology, Seoul National University, Seoul 110-799, Korea
[8]Co-first author
*Correspondence: hyosoo@snu.ac.kr
http://dx.doi.org/10.1016/j.celrep.2015.02.024

SUMMARY

We investigate crosstalk between cancer cells and stromal myeloid cells. We find that Lewis lung carcinoma cells significantly induce PPARβ/δ activity in myeloid cells in vitro and in vivo. Myeloid cell-specific knockout of PPARβ/δ results in impaired growth of implanted tumors, and this is restored by adoptive transfer of wild-type myeloid cells. We find that IL-10 is a downstream effector of PPARβ/δ and facilitates tumor cell invasion and angiogenesis. This observation is supported by the finding that the CD11b^{low}IL-10^{+} pro-tumoral myeloid cell is scarcely detected in tumors from myeloid-cell-specific PPARβ/δ knockout mice, where vessel densities are also decreased. Fatty acid synthase (FASN) is shown to be an upstream regulator of PPARβ/δ in myeloid cells and is induced by M-CSF secreted from tumor cells. Our study gives insight into how cancer cells influence myeloid stromal cells to get a pro-tumoral phenotype.

INTRODUCTION

Tumor-infiltrating myeloid cells are involved in tumor development, progression, and resistance to conventional treatment (Biswas and Mantovani, 2010; Karin et al., 2006; Mantovani et al., 2008; Pollard, 2009) through various mechanisms including mutagenesis, angiogenesis, lymphangiogenesis (Murdoch et al., 2008), suppression of adaptive immunity (Kuang et al., 2009), remodeling of the extracellular matrix, and invasion and metastasis of tumor cells (Lin et al., 2001, 2006). The molecular regulators that determine the diverse pro-tumoral phenotypes of tumor myeloid cells can be an excellent target of a novel anti-cancer therapy. However, the molecular determinants of the diverse pro-tumoral phenotypes in tumor microenvironment have been incompletely understood, though there are several candidates such as NF-kappaB (Hagemann et al., 2008), STAT3 (Kujawski et al., 2008), c-Myc (Pello et al., 2012), and Notch (Wang et al., 2010), mostly for immunosuppressive phenotypes of myeloid cells.

Nuclear receptor peroxisome-proliferator-activated receptor-beta/delta (PPARβ/δ), a key metabolic transcription factor, plays a crucial role in tumorigenesis and tumor progression. However, it is still debated whether PPARβ/δ is pro-tumoral or anti-tumoral (Peters and Gonzalez, 2009; Zuo et al., 2009). Prior work has primarily focused on the role of PPARβ/δ in the malignant cells themselves and not in the tumor stromal cells. Recent two reports suggested that PPARβ/δ might be the key regulator of tumor angiogenesis (Abdollahi et al., 2007; Müller-Brüsselbach et al., 2007). However, the detailed mechanism of PPARβ/δ-dependent tumor angiogenesis has not been elucidated. Tumor-infiltrating myeloid cells have been reported to be most significant cells among the multiple stromal cell types in solid tumors for fostering tumor angiogenesis (Condeelis and Pollard, 2006). Activation of PPARβ/δ regulates anti-inflammatory phenotypes of myeloid cells in other biological contexts such as in atherosclerosis and obesity (Han et al., 2008; Kang et al., 2008; Lee et al., 2003; Odegaard et al., 2008). Thus, we hypothesized that PPARβ/δ activation in myeloid cells of tumor microenvironment would promote its pro-tumoral function to facilitate tumor invasion and angiogenesis.

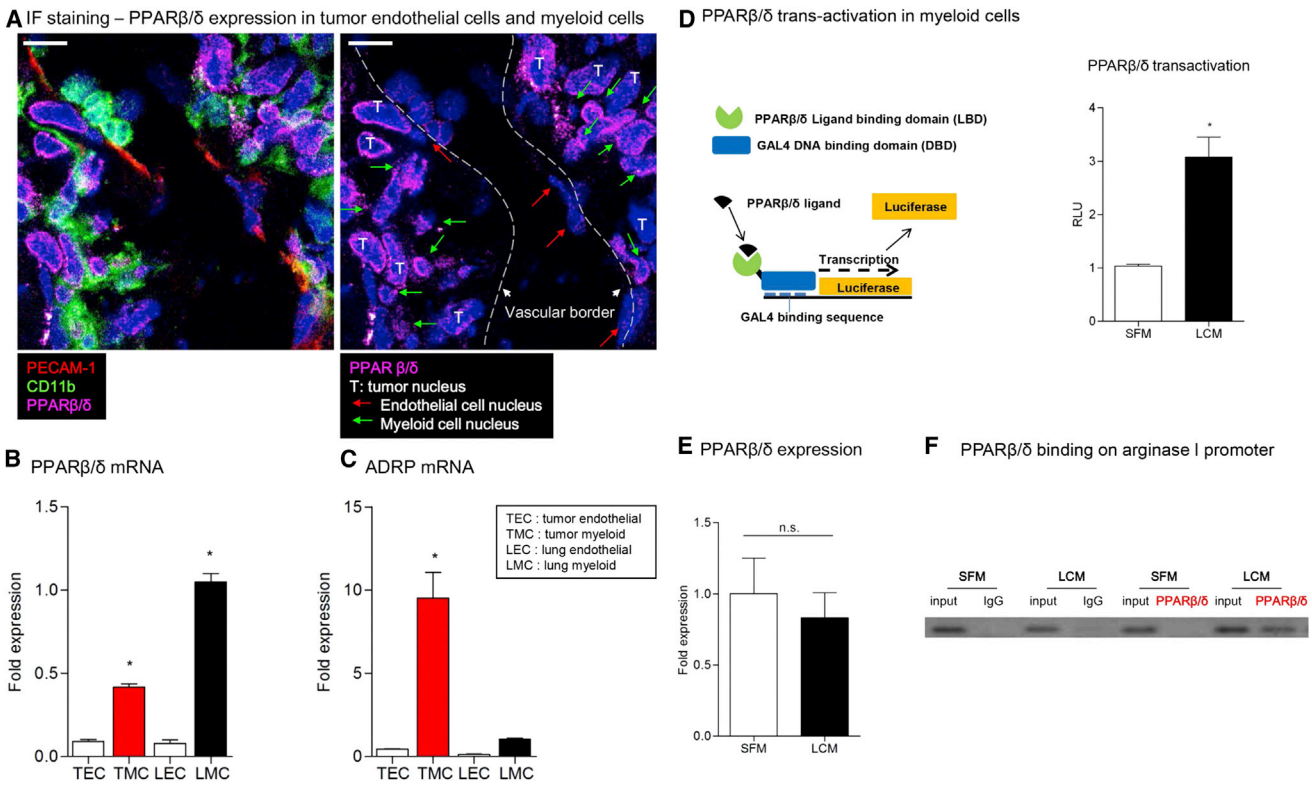

Figure 1. Activation of PPARβ/δ in Myeloid Cells by Lewis Lung Carcinoma

(A) IF staining of tumor tissue from C57BL/6 mice. Blue, nucleus; green, CD11b$^+$ myeloid cells; green arrow, myeloid cell nucleus; magenta, PPARβ/δ; red, CD31$^+$ endothelial cells; red arrow, endothelial cell nucleus; white broken line, capillary wall; scale bars, 10 μm.

(B) PPARβ/δ mRNA expression in endothelial cells (ECs) and myeloid cells (MCs) from LLC tumor (TEC and TMC) and normal lung tissue (LEC and LMC; n = 6). Error bars represent SEM.

(C) ADRP mRNA expression in ECs and MCs from LLC tumor and normal lung tissue (n = 6). Error bars, SEM.

(D) Effect of LCM on PPARβ/δ activation in MC assessed by trans-activation assay (n = 3). PPARβ/δ ligand binds with ligand-binding domain (LBD) and activates GAL4 DNA-binding domain (DBD), which results in luciferase expression. RLU, relative light units. Error bars, SEM.

(E) Effect of LCM on PPARβ/δ mRNA expression in MCs as determined by real-time PCR (n = 8). Error bars, SEM.

(F) Effect of LCM on PPARβ/δ binding at arginase I promoter in MCs as determined by ChiP assay. Representative figure of three independent experiments. See also Figure S1.

RESULTS

Cancer Cells Activate PPARβ/δ in Tumor Myeloid Cells

In mouse model of Lewis lung carcinoma (LLC), PPARβ/δ was substantially expressed in CD11b$^+$ tumor myeloid cells as well as in malignant cells themselves, whereas it was marginally expressed in CD31$^+$ tumor endothelial cells (Figure 1A). Myeloid cells also in other various human cancer tissues showed PPARβ/δ expression, whereas CD31+ endothelial cells rarely expressed it (Figures S1A–S1H). To quantify this observation and to evaluate the activity of PPARβ/δ, we measured the expression and activity of PPARβ/δ in myeloid cells and endothelial cells isolated from tumors and normal lung tissue (Figures S1I and S1J). The expression of PPARβ/δ in myeloid cells was higher than that of endothelial cells. Its expression in myeloid cells was different depending on tissue, lower in lung cancer than in normal lung (Figure 1B). However, the activity of PPARβ/δ or expression of ADRP was remarkably higher in tumor myeloid cells than in myeloid cells from normal tissue (Figure 1C). Interesting finding was discrepancy of expression amount versus activity of PPARβ/δ between myeloid cells in lung cancer versus normal lung (Figures 1B and 1C): lower expression amount and higher activity of PPARβ/δ in myeloid cells of lung cancer than ones of normal lung. To identify the mechanism, we tested the effect of conditioned media of LLC cells (LCM) on PPARβ/δ activation in myeloid cells (Raw 264.7) using PPARβ/δ trans-activation assay. LCM-treated myeloid cells significantly increased PPARβ/δ trans-activation (Figure 1D). Chromatin immuno-precipitation assay showed increased binding of PPARβ/δ to the promoter of arginase I, a representative marker of myeloid cell activation, whereas expression of PPARβ/δ itself was not changed by LCM treatment (Figures 1E and 1F).

The Role of PPARβ/δ in Myeloid Cell for Tumor Growth and Angiogenesis

Because prior report suggested that myeloid cells comprise most of the tumor infiltrates that derived from the bone marrow (BM) (Ahn and Brown, 2008), we introduced BM transplantation

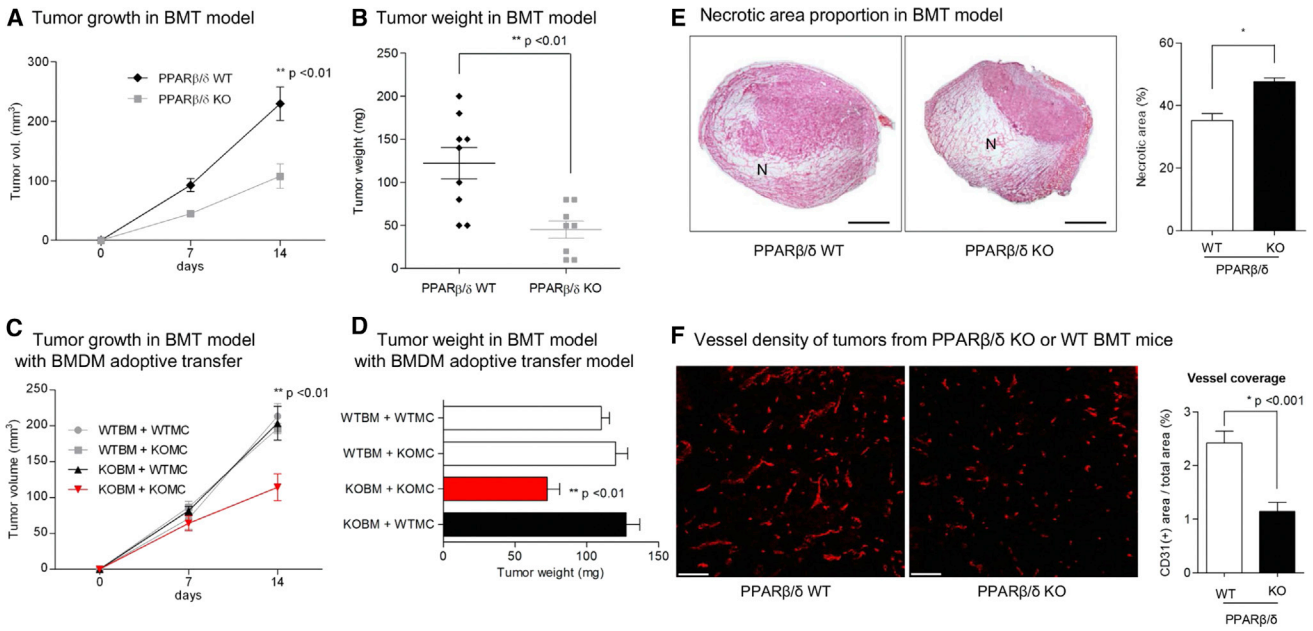

Figure 2. The Role of PPARβ/δ in MCs for Tumor Growth and Angiogenesis

(A) LLC tumor volume growth in PPARβ/δ WT and KO BMT mice (n = 8 or 9 in each group). Error bars, SEM.

(B) LLC tumor weight in PPARβ/δ WT and KO BMT mice at 2 weeks after implantation (n = 8 or 9 in each group). Error bars, SEM.

(C) LLC tumor growth in mice receiving BMT from PPARβ/δ WT or KO mice with adoptive transfer of BMDMs from PPARβ/δ WT or KO mice (n = 4 or 5 in each group). KOBM, PPARβ/δ KO BMT mice; KOMC, adoptive transfer of PPARβ/δ KO BMDMs; WTBM, PPARβ/δ WT BMT mice; WTMC, adoptive transfer of PPARβ/δ WT BMDMs. Error bars, SEM.

(D) LLC tumor weight in PPARβ/δ WT and KO BMT mice with adoptive transfer of PPARβ/δ WT or KO BMDMs (n = 4 or 5 in each group). Error bars, SEM.

(E) Proportion of necrotic area in tumors of mice receiving BMT from PPARβ/δ WT or KO mice. Representative figures of H&E staining of the tumors. N indicates necrotic area. The scale bar represents 1 mm (n = 3 or 4). Error bars, SEM.

(F) CVDs of tumors in mice receiving BMT from PPARβ/δ WT or KO mice. CVDs were determined as the area of CD31 positive per total area (%). The scale bar represents 100 μm (n = 8 in each group). Error bars, SEM.

(BMT) model using PPARβ/δ knockout (KO) or wild-type (WT) BM to test the specific effect of PPARβ/δ activation in myeloid cells. LLC tumor growth was significantly attenuated in mice transplanted with BM from PPARβ/δ KO mice. Tumor volumes in mice receiving BMT from PPARβ/δ WT or KO mice were 229.45 ± 27.93 mm^3 versus 107.94 ± 20.44 mm^3 ($p = 0.0010$) at day 14, and tumor weights were 122.2 ± 18.2 mg versus 45.0 ± 10.2 mg ($p = 0.0028$) at day 14 (Figures 2A and 2B). Our result suggests that PPARβ/δ in myeloid cells is critical in tumor progression. To validate this observation, we performed a reverse experiment by transferring BM-derived myeloid cells (BMDMs) of PPARβ/δ WT or KO mice into mice receiving BMT from PPARβ/δ KO or WT mice along with LLC implantation. Tumors in mice receiving BMT from PPARβ/δ WT mice showed almost the same tumor volume and weight, regardless of the type of the transferred macrophages (WT BMT mice with "WT BMDMs" 213.14 ± 17.57 mm^3 and 110.0 ± 5.7 mg versus WT BMT mice with "KO BMDMs" 195.93 ± 7.25 mm^3 and 120.0 ± 8.6 mg at day 14; Figures 2C and 2D). On the other hand, the tumor growth in mice receiving BMT from PPARβ/δ KO mice remained poor, even after the adoptive transfer of BMDMs from PPARβ/δ KO mice (114.19 ± 18.68 mm^3 and 72.5 ± 8.5 mg at day 14; $p < 0.01$), whereas the attenuated tumor growth in mice receiving BMT from PPARβ/δ KO mice was fully reversed by the adoptive transfer of BMDMs from PPARβ/δ WT mice (203.35 ± 23.50 mm^3 and 127.5 ± 9.5 mg at day 14; Figures 2C and 2D). In addition, it appeared that retarded growth of tumor was associated with broader necrosis in the tumor. The tumor of poor growth in mice receiving BMT from PPARβ/δ KO mice showed larger areas of necrosis in the tumors than those in mice receiving BMT from PPARβ/δ WT mice (KO BMT mice 47.61% ± 1.19% versus WT BMT mice 35.14% ± 2.30%; $p = 0.0034$; Figure 2E). Capillary vessel density (CVD) was also significantly lower in tumor of mice receiving BM from PPARβ/δ KO mice than in those of mice receiving BM from PPARβ/δ WT mice (CVD in KO BMT tumor 1.15% ± 0.17% versus WT BMT tumor 2.42% ± 0.22%; $p = 0.0004$; Figure 2F). This observation supports our hypothesis that PPARβ/δ in tumor myeloid cells has a key role in tumor growth and angiogenesis.

PPARβ/δ Induces Pro-tumoral Phenotype in Tumor Myeloid Cells

To address how PPARβ/δ controls tumor myeloid cells to stimulate tumor growth and angiogenesis, we evaluated the survival, infiltration, and phenotype changes of myeloid cells in tumor microenvironment. In vitro results demonstrated that, when treated with LCM, BMDMs from PPARβ/δ WT or KO mice did not exhibit any difference in survival (Figure 3A). Also, the

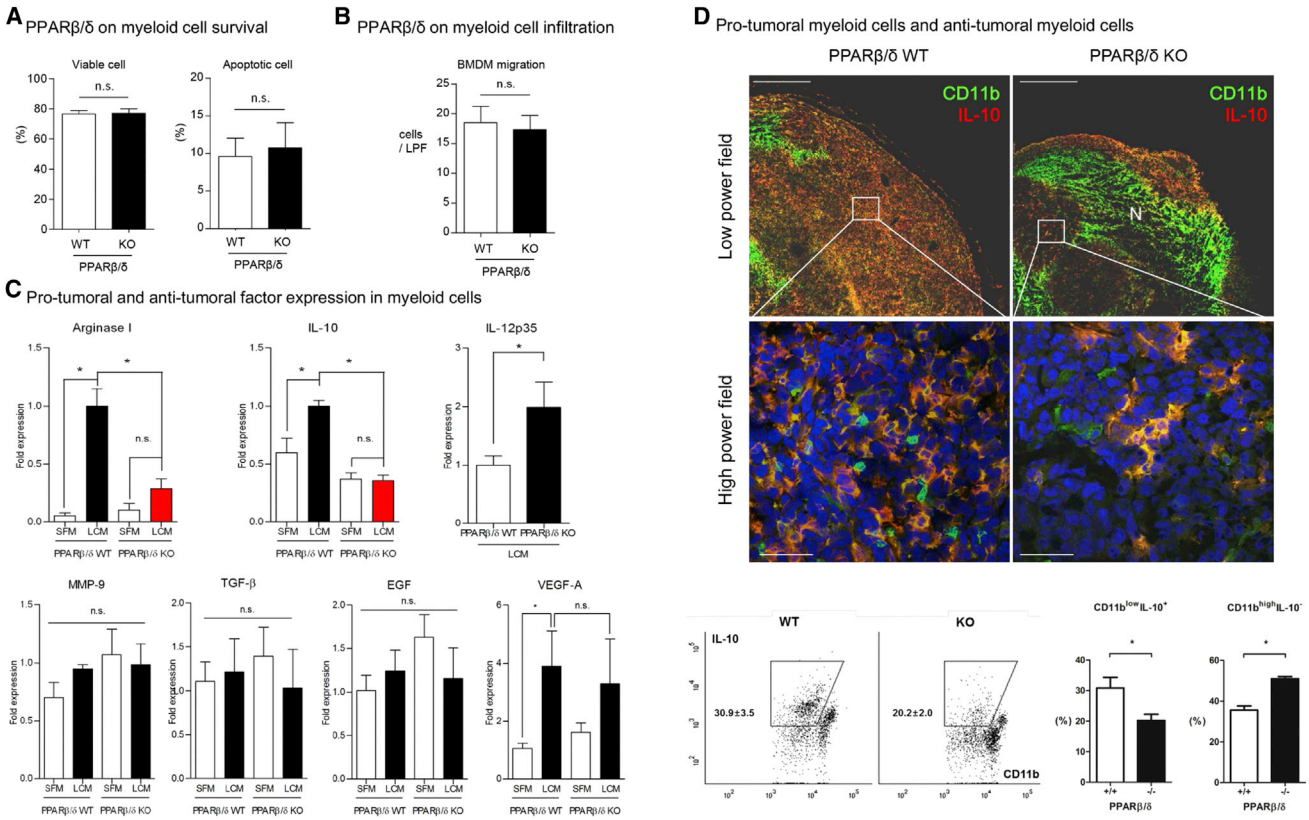

Figure 3. Induction of Pro-tumoral Phenotype in MC by PPARβ/δ

(A) Comparison of PPARβ/δ WT and KO MC survival in vitro. Percentage of viable or apoptotic MC percentage was determined by annexin V/7-AAC staining and FACS analysis. n.s. indicates no significance (n = 4 or 5). Error bars, SEM.

(B) Comparison of PPARβ/δ WT and KO MC infiltration capacity in vitro. MC infiltration capacity was evaluated by transwell migration assay. n.s. indicates no significance (n = 5). Error bars, SEM.

(C) Effect of PPARβ/δ deficiency on expression of pro-tumoral and anti-tumoral factors in MCs treated with serum-free media (SFM) or LLC-cell-conditioned media (LCM). The mRNA expressions of arginase I, IL-10, IL-12p35, VEGF-A, MMP-9, TGF-β, and EGF were determined by real-time PCR (n = 7 for arginase I, IL-10, VEGF-A, and MMP-9; n = 4 for TGF-β and EGF; and n = 11 for IL-12p35). Error bars, SEM.

(D) Distribution and density of $CD11b^{low}IL\text{-}10^{+}$ pro-tumoral MCs in tumor tissues of mice receiving BMT from PPARβ/δ WT or KO mice. Histological sections were stained with antibodies against CD11b (green) and IL-10 (red). N indicates necrotic area. The scale bars represent 500 μm for the upper line and 50 μm for the lower line (n = 8 in each group). $CD11b^{low}IL\text{-}10^{+}$ cells were quantified from FACS analysis of tumors and determined as the percentage of $CD11b^{low}IL\text{-}10^{+}$ cells from total $CD11b^{+}$ MCs; * indicates $p < 0.05$; n = 8 in each group from two independent experiment. Error bars, SEM.

See also Figure S2 and Table S1.

infiltrative capacity of BMDMs toward LLC cells was not affected by PPARβ/δ deficiency (Figure 3B). However, expression of pro-tumoral factors such as arginase I and IL-10 was significantly attenuated in BMDMs of PPARβ/δ KO mice compared with BMDMs of PPARβ/δ WT mice (Figure 3C). Conversely, an important anti-tumoral and anti-angiogenic cytokine, IL-12 was higher in BMDMs of PPARβ/δ KO mice than in those of PPARβ/δ WT mice. Instead, PPARβ/δ deficiency did not affect other well-known pro-tumoral factors such as MMP-9, VEGF-A, TGF-β, and EGF (Figure 3C). NOS2 was similarly produced in WT and KO BMDM (Figure S2). This implies that PPARβ/δ activation induces pro-tumoral phenotype in myeloid cells. These findings were also validated in the tumor tissues of our BMT model. There were two distinct types of $CD11b^{+}$ myeloid cells in the tumor stroma: $CD11b^{low}IL\text{-}10^{+}$ cells and $CD11b^{high}IL\text{-}10^{-}$ cells (Figures S3A–S3C). $CD11b^{low}IL\text{-}10^{+}$ cells or pro-tumoral myeloid cells (Mantovani and Locati, 2009; Mantovani et al., 2002) were more abundant in tumors from PPARβ/δ WT BMT mice compared with those from PPARβ/δ KO BMT mice (Figure 3D). In the tumors from PPARβ/δ WT BMT mice, most of $CD11b^{+}$ cells were $CD11b^{low}IL\text{-}10^{+}$ and they were evenly distributed across the whole tumor tissue without necrosis. In contrast, in the tumors from PPARβ/δ KO BMT mice, there were a larger number of $CD11b^{high}IL\text{-}10^{-}$ cells, which were mostly placed in the necrotic tissue (Figures S3D–S3F). These in vivo results are highly consistent with the in vitro observations and support the conclusion that PPARβ/δ is a key determinant of pro-tumoral phenotype in myeloid cells of tumor. To further characterize the identity of tumor myeloid cells, we performed FACS analysis for lineage markers of $CD11b^{low}IL\text{-}10^{+}$ cells and found that the cells are $F4/80^{+}GR\text{-}1^{-}Ly6G^{-}$ tumor-associated macrophages (Figures 4A and 4B). As IL-10 and arginase I represent M2

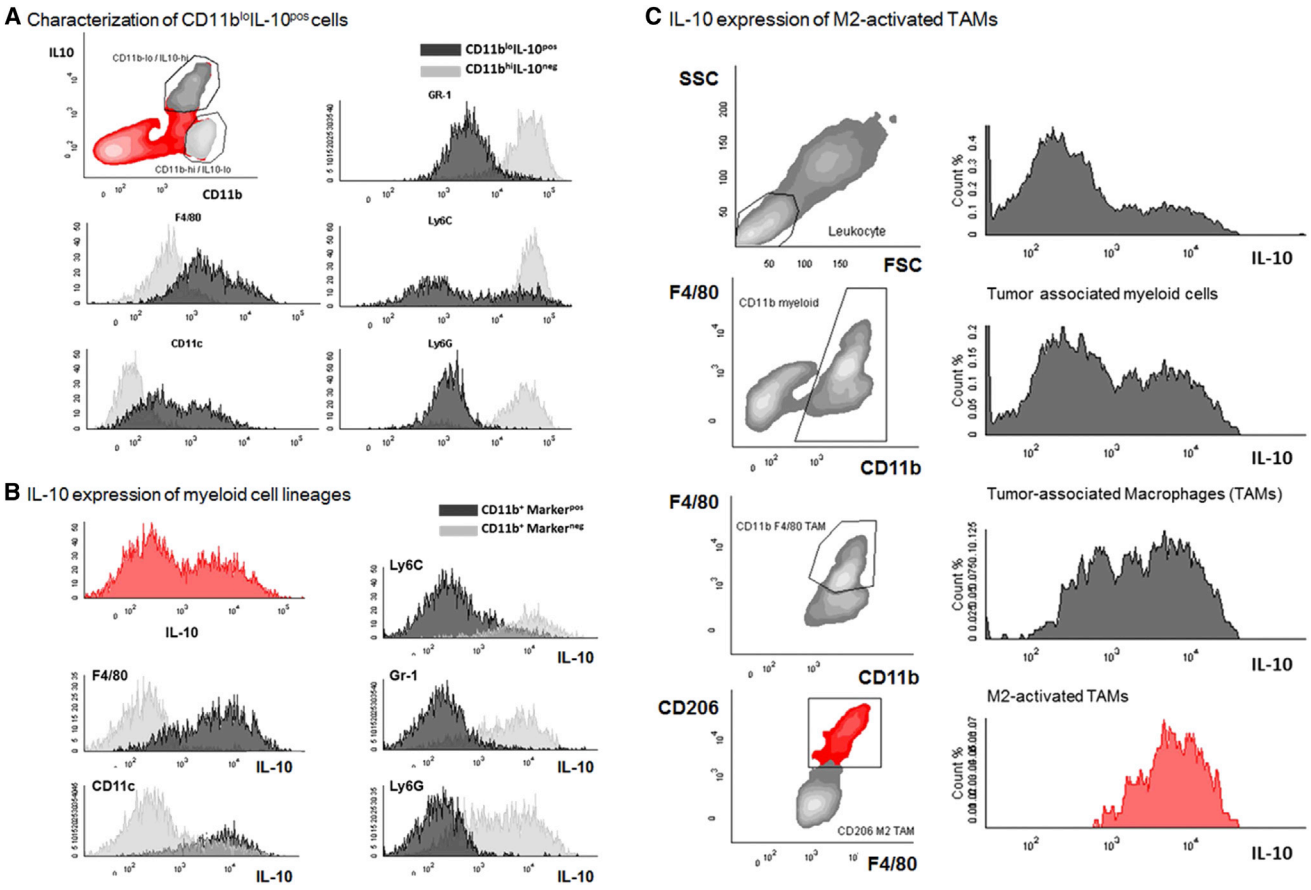

Figure 4. Characterization of IL-10-Producing Tumor MCs

LLC were implanted to wild-type C57 mice. After 2 weeks, the tumors were FACS analyzed for characterization of IL-10-producing tumor MCs.

(A) $CD11b^{low}IL\text{-}10^{+}$ cells were analyzed for lineage markers: GR-1, F4/80, CD11c, Ly6C, and Ly6G (black histogram). The expressions of lineage markers were compared to $CD11b^{high}IL\text{-}10^{-}$ counterpart (gray histogram). Representative result of n = 8 in three independent experiments.

(B) The red-colored histogram represents IL-10 expression of the total $CD11b^{+}$ MCs. The expression of IL-10 in the marker-positive myeloid population (black histogram) is compared to the expression of IL-10 in the marker-negative myeloid population (gray histogram). Representative result of n = 8 in three independent experiments.

(C) Tumor cells were co-stained with IL-10, CD11b, F4/80, and CD206. IL-10 expression (histogram) of the leukocyte gate (top), $CD11b^{+}$ tumor myeloid gate (second row), $CD11b^{+}F4/80^{+}$ tumor-associated macrophage (TAM) (third row) gate and the $CD11b^{+}F4/80^{+}CD206^{+}$ M2-activated TAMs are depicted. Representative result of n = 6 in two independent experiments.

See also Figures S3 and S4.

phenotype of macrophages, we checked additional surface marker of macrophages and found that $CD206^{+}$ M2-activated TAMs represented population with the highest IL-10 expression (Figures 4C and S4A). Those $CD206^{+}$ M2-activated TAMs were mainly located at the non-necrotic area of the LLC tumor and showed increased PPARβ/δ expression (Figures S4B and S4C). Proportion of the M2-activated TAMs was significantly smaller in tumors of the PPARβ/δ KO BMT mice (Figure S4D).

PPARβ/δ Activation in Myeloid Cells Stimulates Cancer Cell Invasion and Angiogenesis in IL-10-Dependent Manner

Then, how does the phenotype of myeloid cells, represented as overexpression of IL-10 by PPARβ/δ (Figure S5), affect tumor cells and tumor angiogenesis? We further evaluated the effect of PPARβ/δ activation and IL-10 upregulation on tumor cell survival, invasion, and angiogenesis in vitro. PPARβ/δ deficiency in BMDMs had no effect on tumor cell apoptosis or survival in co-culture experiment (Figure 5A) but significantly suppressed the tumor cell migration through collagen gel, compared with PPARβ/δ WT BMDMs (Figure 5B). Supplementation of recombinant IL-10 recovered tumor cell invasion that was attenuated by co-culture with PPARβ/δ KO BMDMs, whereas neutralization of IL-10 distinctively blocked tumor cell invasion augmented by co-culture with WT BMDMs (Figure 5C).

In the in vitro assay for tube formation and migration of endothelial cells by co-culture supernatant of tumor cells and BMDMs from either PPARβ/δ WT or KO mice, the angiogenic capacity was significantly decreased in the supernatant from co-culture of PPARβ/δ KO BMDMs and tumor cells, compared with the supernatant from PPARβ/δ WT BMDMs co-cultured with tumor cells. The retarded angiogenic effect of PPARβ/δ KO myeloid

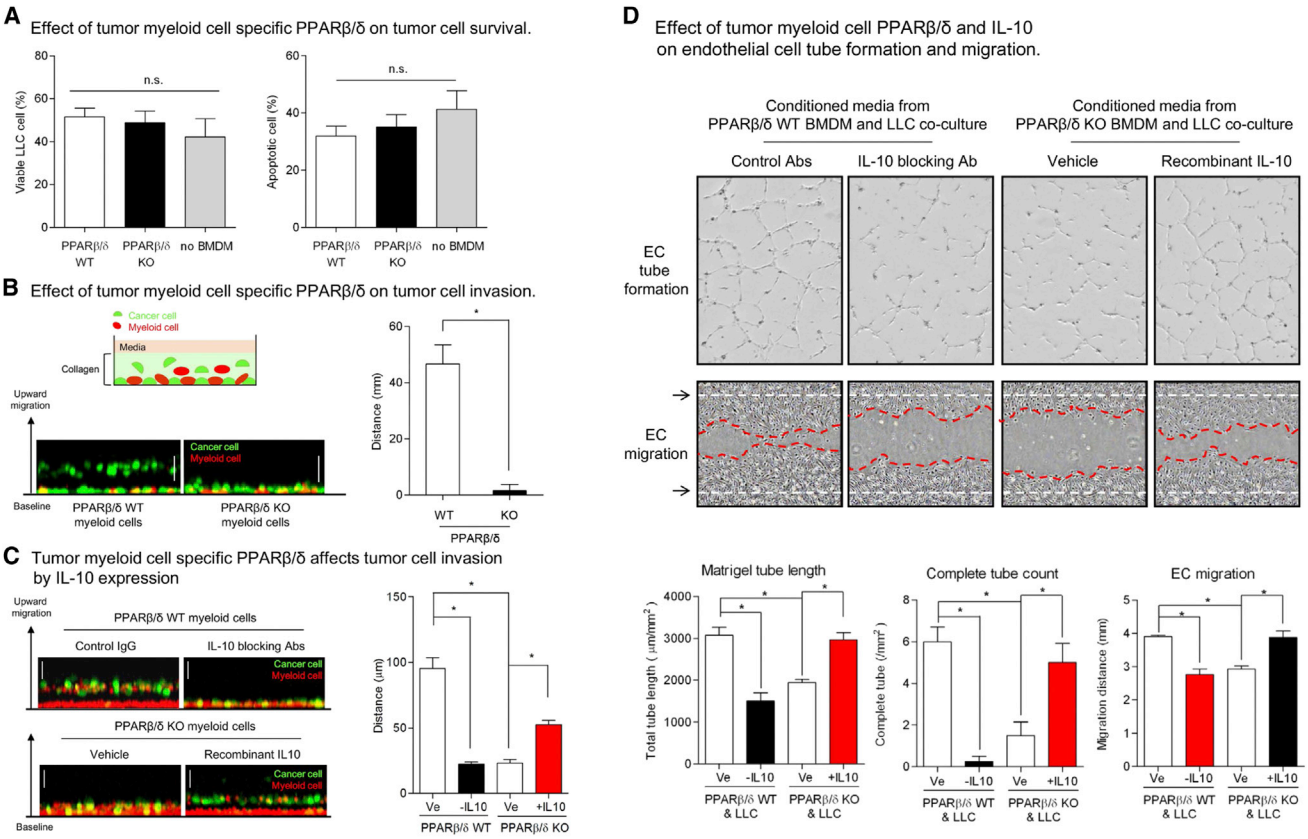

Figure 5. The Mechanism of Pro-tumoral MCs to Enhance Tumor Cell Invasion and Angiogenesis

(A) Effect of myeloid-cell-specific PPARβ/δ on tumor cell survival. Percentage of viable or apoptotic MC percentage was determined by annexin V/7-AAC staining and FACS analysis. n.s. indicates no significance (n = 4). Error bars, SEM.

(B) Effect of myeloid-cell-specific PPARβ/δ on tumor cell invasion. Tumor cell invasion capacity was evaluated by collagen gel invasion assay as described in schematic illustration. Green cell indicates GFP-tagged 3LL tumor cells, and red cell indicates PKH-Red-tagged BMDMs. The scale bar represents 50 μm (n = 3). Error bars, SEM.

(C) IL-10-mediated effect of myeloid-cell-specific PPARβ/δ on tumor cell invasion. Abs indicates antibodies. Green cell indicates 3LL tumor cells (GFP tagged), and red cell indicates PKH-Red-tagged BMDMs. Ve indicates control IgG or vehicle. The scale bar represents 50 μm (n = 3 or 4). Error bars, SEM.

(D) IL-10-mediated effect of myeloid-cell-specific PPARβ/δ on EC tube formation and migration. EC tube formation in Matrigel was determined by total tube length (μm) or complete tube counts per area (/mm^2). EC migration function was tested by scratch-wound assay, and migration potential was determined by average of migration distance (mm). Ve indicates control IgG or vehicle (n = 6). Error bars, SEM.

See also Figure S5.

cells was rescued by the supplementation of recombinant IL-10, whereas normal angiogenic effect of PPARβ/δ WT myeloid cells was attenuated by the neutralization of IL-10 (Figure 5D). These results demonstrate that IL-10 is the key mediator of PPARβ/δ-dependent function of myeloid cells in tumor microenvironment, promoting tumor cell invasion and tumor angiogenesis.

Mechanism How Cancer Cells Activate PPARβ/δ in Myeloid Cells: Paracrine Network Involving M-CSF and FASN

Using arginase I mRNA expression as a marker, we screened possible endogenous ligands of PPARβ/δ in tumor microenvironment: free fatty acids; prostaglandins; and arachidonic acids. Because the ligands could originate from either cancer cells (exogenously) or myeloid cells (endogenously), we treated the inhibitors of each enzyme to cancer cells before LCM preparation or directly to BMDMs (Figure S6A). Here, only fatty acid synthase (FASN) inhibitor directly treated to myeloid cells blocked arginase I upregulation caused by LCM (Figure 6A). To verify this result, we made FASN knockdown LLC cells and FASN knockdown myeloid cells (Raw 264.7) using sh-FASN lentivirus (Figures S6B and S6C) and observed that LCM-induced PPARβ/δ activation is blocked by FASN knockdown in myeloid cells, but not by FASN knockdown in cancer cells (Figure 6B). In agreement with this finding, FASN expression was significantly increased in myeloid cells by LCM (Figures 6C and 6D). This result implies that endogenous ligands derived from FASN in myeloid cells can be a key regulator of PPARβ/δ activity in the context of tumor myeloid cells.

Then, to find the candidate messengers in tumor microenvironment that mediates FASN expression and PPARβ/δ activation in myeloid cells, we analyzed LCM regarding several secretary

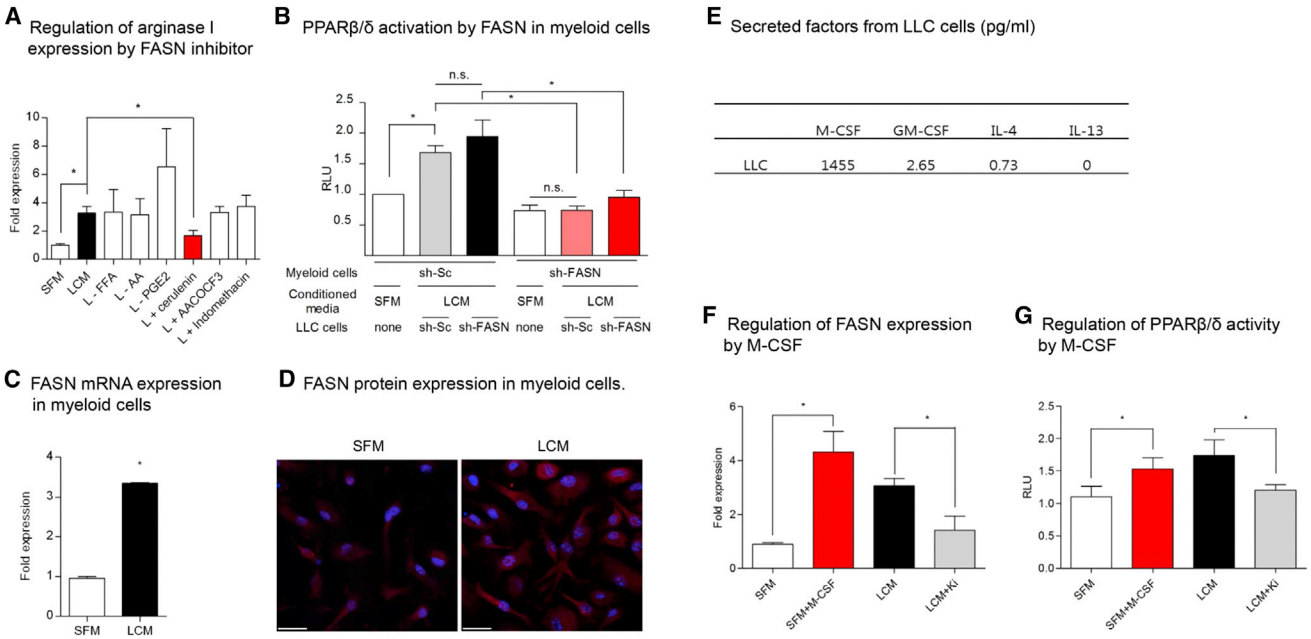

Figure 6. Paracrine Mechanism How Tumor Cells Activate PPARβ/δ in MCs

(A) Arginase I expression in MC after blocking the production of free fatty acids (FFAs), arachidonic acids (AAs), or prostaglandins (PGs) in LLC cells and MCs by inhibitor of FASN, cPLA2, or COX (n = 4–7). L−AA, AAs-depleted LCM; L+AACOCF3, LCM supplemented with AACOCF3; L+cerulenin, LCM supplemented with cerulenin; L−FFA, FFAs-depleted LCM; L+indomethacin, LCM supplemented with indomethacin; L−PG, PG-depleted LCM. *indicates $p < 0.05$. Error bars, SEM. Detailed scheme of the experiment is described in Figure S6.

(B) Effect of FASN knockdown in LLC cells or MCs on PPARβ/δ activation in MC determined by trans-activation assay (n = 4–6). FASN was knockdown by sh-*FASN* lentiviral transduction into LLC cells or Raw 264.7 MCs, and sh-*scramble* (sh-Sc) lentivirus was used as control. * indicates $p < 0.05$. Error bars, SEM.

(C) Effect of LCM on FASN expression in MCs (n = 3). * indicates $p < 0.05$. Error bars, SEM.

(D) IF staining against FASN in MCs cultured in SFM or LCM. LCM significantly induced FASN protein expression in MCs. Representative figure of three independent experiments. The scale bars represent 20 μm.

(E) Analysis of LCM regarding tumor-derived factors that are known to be involved in activation of MCs using ELISA, pg/ml (n = 3).

(F) Effect of M-CSF (50 ng/ml) or M-CSF receptor inhibitor Ki20227 (1 μM) on FASN expression in MCs, by real-time PCR. M-CSF as well as LCM significantly increased FASN mRNA expression in MCs, and Ki20227 reversed the effect of LCM (n = 4–6). * indicates $p < 0.05$. Error bars, SEM.

(G) Effect of M-CSF (50 ng/ml) or M-CSF receptor inhibitor Ki20227 (1 μM) on PPARβ/δ activity in MCs, by PPARβ/δ trans-activation assay. M-CSF as well as LCM significantly activated PPARβ/δ in MCs, and Ki20227 reversed the effect of LCM (n = 3 or 4). * indicates $p < 0.05$. Error bars, SEM.

See also Figures S6 and S7.

factors that have been shown to be important in activation of macrophages or PPARβ/δ. We found that macrophage colony-stimulating factor (M-CSF) was markedly secreted by LLC cells (Figure 6E), and FASN expression was significantly increased by M-CSF treatment in myeloid cells, whereas blocking M-CSF in LCM with Ki20227, a specific inhibitor of M-CSF receptor, reversed the induction of FASN expression by LCM treatment (Figure 6F). Moreover, M-CSF treatment resulted in PPARβ/δ activation in trans-activation assay, whereas PPARβ/δ activation by LCM was blocked by Ki20227 (Figure 6G). These results altogether indicate that M-CSF secreted from LLC cells induces FASN expression in myeloid cells, leading to PPARβ/δ activation.

DISCUSSION

Here, we demonstrate that PPARβ/δ activation in tumor myeloid cells control their pro-tumoral phenotype, particularly the expression of IL-10, and stimulates tumor angiogenesis and matrix invasion of malignant cell. The physiological relevance of this pathway was demonstrated in LLC tumor model with PPARβ/δ WT and KO BMT mice, which revealed that PPARβ/δ deficiency in tumor myeloid cell attenuated tumor growth and angiogenesis. Finally, we found that PPARβ/δ activation in tumor myeloid cells was induced by the paracrine network between M-CSF from cancer cells and induction of FASN in myeloid cells.

Importance of PPARβ/δ in Myeloid Cells to Control Tumor Growth

Previous studies of PPARβ/δ in cancer paid attention exclusively to the role of PPARβ/δ in malignant cells and carcinogenesis (Gupta et al., 2004; Peters and Gonzalez, 2009; Peters et al., 2008). But there have been two studies that distinguished the effect of PPARβ/δ in malignant cells from stromal cells and evaluated the effect of PPARβ/δ in tumor stromal cells. In both studies, they made tumor model with PPARβ/δ WT/KO mice implanted with syngeneic PPARβ/δ WT LLC cells. Then they showed that PPARβ/δ-deficient stromal cells delayed tumor growth and attenuated functional tumor angiogenesis (Abdollahi et al., 2007; Müller-Brüsselbach et al., 2007). However, the two studies focused only on tumor endothelial cells based on

previous reports on the role of PPARβ/δ in endothelial function. (Brunelli et al., 2007; Fan et al., 2008; Ghosh et al., 2007; Liou et al., 2006; Piqueras et al., 2007). Here, we found that the expression and the activity of PPARβ/δ were lower in tumor endothelial cell compared to tumor myeloid cell. In vivo tumor model of PPARβ/δ WT or KO BMT mice and adoptive transfer of PPARβ/δ WT or KO myeloid cells demonstrated that PPARβ/δ in myeloid cell is critical in tumor growth and angiogenesis. Our study also suggests that the difference of tumor angiogenesis in PPARβ/δ WT and KO mice is a result of altered phenotype of tumor myeloid cells. It provides strong evidence that PPARβ/δ plays a significant role in stromal cells, especially in tumor myeloid cell, and gives us further insight of the molecule's role in tumor angiogenesis.

Importance of PPARβ/δ in Myeloid Cells to Induce M2-like Pro-tumoral Phenotype

Previous studies argue that the immune suppressive and angiogenic phenotype of infiltrating myeloid cells are crucial determinants of tumor progression (Condeelis and Pollard, 2006; Pollard, 2004). Classically, the phenotype was simply classified into M1, the pro-inflammatory microbactericidal and tumoricidal phenotype, and M2, the immune-regulatory phenotype involved in tissue remodeling and tumor progression (Sica and Mantovani, 2012). Tumor-associated monocytes-macrophages are roughly considered to present M2-like phenotype, which is associated with the promotion of tumor growth and tissue remodeling (Galdiero et al., 2013). In present study, BMDMs treated with LCM increased expression of IL-10, arginase I, and VEGF whereas decreased expression of IL-12. Induction of IL-10 and arginase I as well as suppression of IL-12 were PPARβ/δ-dependent, whereas induction of VEGF was not dependent on PPARβ/δ. ChiP result confirmed that LCM increased binding of PPARβ/δ to PPRE of arginase I. To our knowledge, this is the first report investigating the role of PPARβ/δ regulating the M2-like pro-tumoral phenotype of tumor-associated myeloid cells.

IL-10 dampens the immune response to pathogens and is a well-known anti-inflammatory product of T-helper 2 cells (Saraiva and O'Garra, 2010). In tumor, the increased production of IL-10 from myeloid cells promotes immune suppression through activation of STAT3 (Kinjyo et al., 2006; Kujawski et al., 2008). In another report, IL-10-producing LLC cell line showed more rapidly growing tumor with increased vessel density in mice compared to control (Dace et al., 2008; Mocellin et al., 2003; Zeng et al., 2010). In vitro result of our study suggests that IL-10 might exert direct effect on endothelial cell migration and tube formation. Overall, pro-tumoral effect of IL-10 seems to be mediated not only by suppression of immune surveillance against tumor but also by enhancement of angiogenesis.

Upstream Regulator of PPARβ/δ in Myeloid Cells

Several eicosanoids and saturated and unsaturated fatty acids were suggested to be natural ligands of PPARβ/δ (Forman et al., 1997; Krey et al., 1997; Xu et al., 1999; Yu et al., 1995). PPARβ/δ activation in myeloid cells has been described in previous reports. The suggested relevant ligands of PPARβ/δ included VLDL-particle-derived fatty acids (Chawla et al., 2003), adipose-tissue-derived fatty acids (Odegaard et al., 2008), and apoptotic-cell-derived fatty acids (Mukundan et al., 2009). All the previous reports focused on exogenous ligands and the potential mechanism to transport the ligands to the cytoplasm of myeloid cell. Because increased production of de novo fatty acids was known as a hallmark of cancer cell transformation (Menendez and Lupu, 2007), we initially postulated that fatty acids derived from cancer cells would act as a significant mediator of interaction between myeloid cells and tumor. Unexpectedly, FASN knockdown in LLC did not exert any effect on PPARβ/δ activation in myeloid cells. Instead, FASN knockdown in myeloid cells themselves significantly reduced PPARβ/δ activation by the LCM. This provides the first evidence that "endogenous FASN" in myeloid cell is necessary for the activation of PPARβ/δ in tumor myeloid cell. In colorectal carcinoma, endogenously synthesized prostaglandin I_2 and 13-S-hydroxyoctadecadienoic acid were reported to modulate PPARβ/δ activity (Gupta et al., 2000; Shureiqi et al., 2003). Recently, the importance of FASN and endogenously synthesized "new fat" was highlighted in mouse liver to activate another PPAR family. In the report, FASN was shown to produce long-chain fatty acid, which was then converted to specific endogenous ligand to activate PPARα (Chakravarthy et al., 2009). In this regard, we suggest that FASN-derived new fat or its derivatives may activate PPARβ/δ. Further study is needed to identify the physiologically relevant endogenous ligand of PPARβ/δ in myeloid cells.

Mechanism of Cancer Cells to Tame Myeloid Cells: Paracrine Network Involving M-CSF to FASN

TAMs, in terms of metabolism, are expected to downregulate FASN expression due to carbohydrate deprivation from excessive glucose utilization by the surrounding malignant cancer cells. In this regard, we speculate that the M-CSF signaling plays the critical role in the unexpected upregulation of FASN in TAMs. Previous studies reported the role of cancer-derived M-CSF in the differentiation of myeloid cell phenotype. M-CSF is the key cytokine that induces myeloid cell to have the immunosuppressed and tissue-trophic phenotype (Mantovani et al., 2002; Pollard, 2004). The signal pathways activated by M-CSF include PI3K/Akt, MAPK, and JAK/STAT pathway (Mouchemore and Pixley, 2012). These are the same pathways reported to be responsible for the dysregulated overexpression of FASN in malignant cells (Menendez and Lupu, 2007). Regarding downstream effectors, M-CSF stimulated production of IL-10 and CCL2 whereas suppressing IL-12 and IL-23 (Fleetwood et al., 2007; Lacey et al., 2012). However, the exact mechanism how M-CSF regulates wide range of downstream effectors is still uncovered. In the present study, M-CSF from cancer cells increased the expression of FASN and activated PPARβ/δ to increase IL-10 expression and suppress IL-12 expression.

Generalization and Application

We asked whether the above finding was generalizable to different solid tumors. When we compared the growth of various cancer cell lines in PPARβ/δ WT and KO BMT mice (Figure S7A), only the B16-F10 melanoma cell line showed impaired tumor growth like LLC cell line. Interestingly, only the supernatants of LLC and B16-F10 upregulated the expression of FASN and subsequently increased the PPARβ/δ activity of myeloid cells in vitro

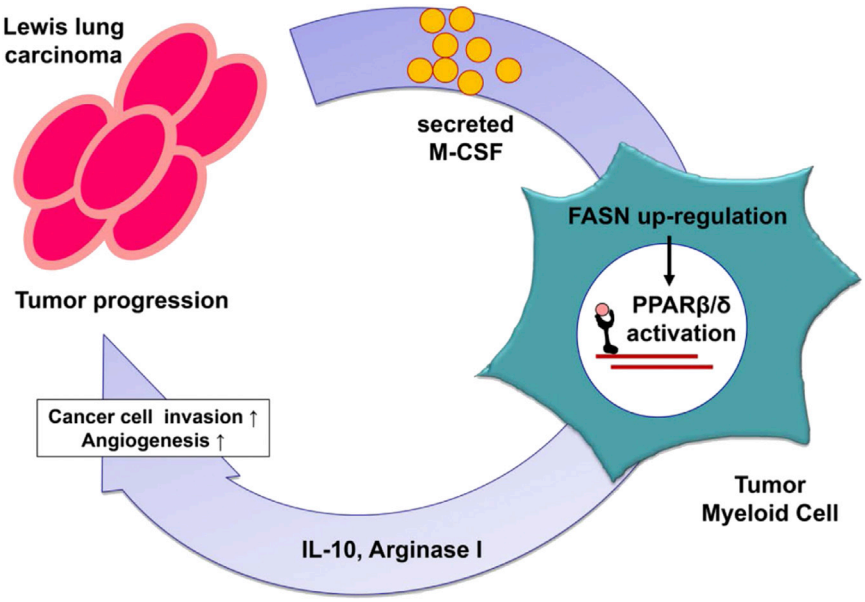

Figure 7. Crosstalk between Tumor and Stromal Cells in Tumor Microenvironment

M-CSF secreted from tumor cells induces FASN in MCs, leading to PPARβ/δ activation, phenotypic change, and secretion of IL-10 from MCs. IL-10 from MCs in turn stimulates tumor cell invasion as well as angiogenesis by ECs migration and proliferation.

(Figures S7B and S7C). We speculate that there might be a specific phenotype of cancer that influences tumor myeloid cells via the FASN-PPARβ/δ pathway. As synthetic antagonist of PPARβ/δ is available, characterization of the specific phenotype and its marker in human cancer would be a promising strategy to target the tumor microenvironment and impair cancer progression.

Taken as a whole, the present study identifies a new liaison between malignant cells and stromal cells. M-CSF from cancer cells induces FASN-PPARβ/δ pathway in stromal cells, leading to secretion of IL-10 and tumor progression (Figure 7).

EXPERIMENTAL PROCEDURES

Animal Experiments

We used PPARβ/δ KO mice with the exon 8 of the gene disrupted as previously described (Peters et al., 2000). BM cells were isolated from PPARβ/δ WT or KO mice and underwent lineage depletion (CD3, CD11b, CD45R/B220, Gr-1, and TER119; BD Biosciences) with magnetic-activated cell sorting (MACS) (Miltenyi Biotec). Recipient mice received lethal dose of 6.5 + 6.5 Gy irradiation with 4-hr interval. Lineage-depleted hematopoietic stem cells (1×10^5 cells/ recipient) were injected into recipient mice within 24 hr after the second irradiation. Donor marrow was allowed to repopulate for 4 weeks, and the mice were used for LLC tumor model. All the animal protocol was approved by the Experimental Animal Committee of Seoul National University. 7×10^5 LLC cells at exponential growth were suspended in 70 μl of growth-factor-reduced Matrigel (BD Biosciences) and injected subcutaneously in the left flank of indicated mice. For adoptive transfer experiments, equal number of PPARβ/δ WT or KO BMDMs were mixed with LLC cells in 70 μl of Matrigel. Tumor sizes (length [L] and width [W]) were measured using calipers, and tumor volume was calculated using the equation volume = $L \times W^2/2$. Tumor was dissected, and the weight was measured 2 weeks after implantation. All the animal experiments of the study were approved by the Institutional Animal Care and Use Committee (IACUC) in Seoul National University Hospital (IACUC approval no. SNU-140630-4).

Sorting of Endothelial Cells and Myeloid Cells from LLC Tumor and Normal Lung Tissue

Two weeks after LLC cells were injected into Tie-2 GFP transgenic mice as above, tumors were surgically removed, minced, and digested with collagenase I (1 mg/ml) and DNase I (1 mg/ml; Roche) in HBSS for 30 min at 37°C and passed through 40-μm cell strainer. Dissociated single cells were stained with CD11b-APC antibody (BD Biosciences) and sorted with FACSAria based on their fluorescence (GFP: Tie-2^+ endothelial cells; PerCP: $CD11b^+$ myeloid cells; Figure S2).

Macrophage Isolation and Culture in Conditioned Media

BMDMs were isolated and cultured as described previously (Weischenfeldt and Porse, 2008). Briefly, marrow was flushed from femur and tibia of indicated mice, passed through 40-μm cell strainer, and incubated in hypotonic RBC lysis solution. The cells were plated at a density of 1×10^6/ml and cultured in RPMI containing 10% FBS and 15% L-929-conditioned media for 7 days. At day 8, differentiated macrophages were used for subsequent experiments. LCM was prepared as previously described (Kim et al., 2009). Briefly, 12 hr after 2×10^6 LLC had been plated on a 10-cm culture dish, growth media was replaced by 8 ml of serum-free RPMI 1640. The conditioned media was collected for next 18 hr, centrifuged for 10 min at 3,000 g, and passed through 0.45-μm pore filter. Serum-free RPMI 1640 medium (SFM) was incubated for the same duration and passed through the filter to serve as control media. SFM and LCM were treated for 18 hr to evaluate macrophage phenotype gene and PPAR β/δ expression and for 8 hr for FASN expression and ChIP assay. To block each enzyme activity of LLC during LCM preparation, the following concentrations of inhibitors were treated to LLC cells 1 hr before the start of LCM preparation: cerulenin (5 μg/ml; Sigma-Aldrich); AACOCF3 (10 μM; Tocris Bioscience); and indomethacin (1 μM; Sigma-Aldrich). To block the enzyme activities of BMDM during LCM stimulation, the same concentration of each inhibitor was mixed to the LCM.

Immunofluorescence Staining of Tumor Tissue and BMDM

The tumor tissues were embedded in OCT compound and frozen in isopentane cooled with liquid nitrogen. The frozen tissue was cut into 8-μm section and fixed with acetone or 1% PFA. Blocking was done with 5% normal goat serum with 1% BSA and 1% FcR blocker (Miltenyi Biotec). Rat anti-CD31 antibodies, rat anti-IL-10 antibodies (eBioscience), rabbit anti-PPAR β/δ antibodies (Santa Cruz Biotechnology), biotinylated anti-CD11b antibodies (BD Biosciences), and FITC-tagged anti-CD31 antibodies (BD Biosciences) were used as primary antibodies. The nuclei were counterstained with Sytox blue (Invitrogen). To evaluate CVDs, CD31-positive area per total area was quantified at six random fields of each section. To quantify $CD11b^{low}IL\text{-}10^+$ cells infiltration, $IL\text{-}10^+$ cells were automatically counted and manually confirmed to be $CD11b^{low}$. LSM 710 microscopes and ZEN 2010 Software (Carl Zeiss) were used for image acquisition and Image-Pro Plus (MediaCybernetics) for quantification.

FACS Analysis of Tumor-Infiltrating Myeloid Cells

Tumors of LLC injected into PPARβ/δ WT or KO BMT mice were prepared to single-cell suspension as described above at 2 weeks. FITC-tagged anti-CD11b; PE-tagged anti-IL-10; PerCP-Cy5.5-tagged anti-F4/80; and APC-tagged anti-Ly6C, anti-Ly6G, anti-CD11c, anti-CD86, anti-MHC class II, and anti-CD206 antibodies were used for analysis.

Annexin V and 7-AAD FACS Analysis for Cell Survival

BMDMs were tagged with PKH-26 kit (Sigma-Aldrich) according to manufacturer's protocol to distinguish it from LLC cells during the co-culture experiments. Equal number of BMDMs and LLC cells (each 3 × 10^5 cells) were co-cultured for 24 hr in SFM. The co-cultured cells were stained with annexin V-FITC and 7-AAD, and the percentage of apoptotic and necrotic cells were quantified with FACS Canto-II (BD Biosciences). LLC cells and BMDMs were separately gated based on PKH-26 signal (585/42 [PE] detector). The percentage of apoptotic (annexin V-FITC; 530/330 [FITC] detector) and necrotic/late apoptotic (7-AAD; 670LP [PerCP-Cy5.5, PERCP] detector) cells were calculated in each gate. For experiments of PPARβ/δ WT or KO BMDM survival, the BMDMs were cultured for 24 hr in SFM, stained with annexin V-FITC and 7-AAD, and analyzed as above except for PE gating.

Invasion/Infiltration Assay

The 24-well insert system (BD Biosciences) was used to assess BMDM infiltration capacity. LLC cells and PKH-26-stained BMDMs were plated in 24-well bottom plate and on 8-μm pore inserts, respectively. After 12 hr, the inserts were placed on the LLC culture. After 24 hr, BMDM infiltration was quantified as the red fluorescent cell counts at the bottom of the insert.

For the assessment of LLC cell invasion capacity affected by BMDMs, we modified previously described vertical collagen gel chamber invasion assay (Yoon et al., 2005). GFP-tagged LLC cells were added on PKH-26-stained BMDMs already plated on optical 8-well dish (Ibidi). The co-cultured cells were then covered with 150 μl of collagen (Millipore) and GFR-reduced Matrigel (BD Biosciences) mixture (1:1) and kept at 37°C until the gel polymerized. After 1 hr, 100 μl of RPMI 10% FBS medium was added on the top of collagen gel to attract the cells upward in each well. The vertical upward migration of green (LLC) and red (BMDM) cells were quantified using the z stack imaging acquired with Zeiss LSM 710 confocal microscopy.

Endothelial Cell Function Assay

Matrigel tube formation (Hur et al., 2007) and scratch wound assay (Lee et al., 2009) were done as previously described with slight modification of the protocol. For tube formation, 2 × 10^4 human umbilical vein endothelial cells (Lonza) were seeded on the Matrigel-coated chamber slide with indicated conditioned media treated with recombinant mouse IL-10 (10 ng/ml), anti-IL-10-blocking antibodies (eBioscience; 0.5 μg/ml), or protein/antibody control. After 12 hr, four random fields were taken and the count of complete tube formation per unit area and total length of tube in the field were quantified. For migration assay with scratch-wound model, MS1 (mouse endothelial cell line; ATCC) cells were cultured in 6-well dishes to confluence. The monolayers were scraped through the middle of the dish by using a sterile disposable rubber policeman. After wounding, monolayers were immediately washed and incubated with indicated conditioned media and recombinant mouse IL-10 (10 ng/ml), anti-IL-10-blocking antibody (0.5 μg/ml), or protein/antibody control. After 24 hr, migration of the cells was quantified by measuring average distance of maximal migration into denuded area at five points of regular interval. Image-Pro Plus was used for quantification.

PPARβ/δ Trans-activation Assay

The ligand-binding domain of mouse PPARβ/δ was fused to the DNA-binding domain of the yeast transcription factor Gal4 under the control of the SV40 promoter, and the plasmid also encoded the UAS-firefly luciferase reporter under the control of the Gal4 DNA response element (Bility et al., 2004). Monomacrophage cell line RAW 264.7 was transfected with plasmid DNA used with Neon electroporation system (Invitrogen; Guignet and Meyer, 2008). The electroporation condition was 3 × 10^5 cells in 10 μl with single pulse of voltage 1,680 V over 20 ms. 6 × 10^5 cells from two electroporations were pooled and plated on a 6-well dish with media supplemented with 20% FBS and 15% L-media. After 24 hr of stabilization, the transfected cells were treated with different conditioned media for 24 hr and the luciferase activity was measured. As the reporter produced firefly luciferase, we used constitutively expressed *Renilla* luciferase (pRL-TK; Promega) for transfection control and quantified luciferase activity with dual luciferase assay kit (Promega) according to manufacturer's protocol.

FASN Knockdown with Short-Hairpin Lentivirus

To reduce endogenous FASN expression, pLL3.7 lentiviral vector (Addgene) that expresses shRNA under the mouse U6 promoter was utilized. A CMV-EGFP reporter cassette is included in the vector to monitor expression. We followed previous protocol to produce lentiviral vectors (Rubinson et al., 2003). The consensus sequences were provided by The RNAi Consortium. The sequence for FASN knockdown was 5′-GCTGGTCGTTTCTCCATTAAA-3′ and shRNA sequence for scramble (Sc) control was 5′-CAACAAGATGAAG AGCACCAA-3′. Sub-confluent RAW 264.7 and LLC cells were transducted with indicated lentivirus and limit diluted in 96-well to get the single clone with consistent GFP expression. The resulting clones were expanded, and the FASN knockdown was confirmed with real-time PCR.

Statistical Analysis

All data are presented as mean ± SE. Student's t test or paired t test was performed for inter-group comparisons. One-way ANOVA with Bonferroni correction was used for multiple-group comparisons. SPSS version 16.0 was used for analysis, and a p value of <0.05 was considered statistically significant.

See also Supplemental Experimental Procedures.

SUPPLEMENTAL INFORMATION

Supplemental Information includes Supplemental Experimental Procedures, seven figures, and one table and can be found with this article online at http://dx.doi.org/10.1016/j.celrep.2015.02.024.

AUTHOR CONTRIBUTIONS

J.P. provided execution of experiments, data analysis and interpretation, and drafting of the manuscript; S.E.L. provided conception and design of experiments, data analysis and interpretation, and drafting of the manuscript; J.H. provided execution of experiments, data analysis and interpretation, and drafting of the manuscript; E.B.H. provided execution of experiments and data analysis; J.-I.C. provided execution of experiments and data analysis; J.-M.Y. provided data analysis and interpretation and critical review of the manuscript; J.-Y.K. provided execution of experiments, data analysis and interpretation, and critical review of the manuscript; Y.-C.K. provided data analysis and interpretation and critical review of the manuscript; H.-J.C. provided conception and design of experiments and critical review of the manuscript; J.M.P. provided data analysis and interpretation and critical review of the manuscript; S.-B.R. provided key experiment materials and critical review of the manuscript; Y.T.K. provided key experiment materials and critical review of the manuscript; and H.-S.K. provided conception and design of experiments, data analysis and interpretation, and critical review of the manuscript.

ACKNOWLEDGMENTS

We thank Ms. H.W. Jung for her excellent assistance in animal experiments. This study was supported by grants from the Bio & Medical Technology Development Program (2010-0020258) of Korea National Research Foundation (NRF); the Innovative Research Institute for Cell Therapy (A062260) funded by Ministry of Health & Welfare (MHW); and the Korea Health Technology R&D Project (HI12C16910000, HI14C1277, and HI12C0199) through the Korea Health Industry Development Institute, funded by MHW.

Received: May 13, 2014
Revised: January 6, 2015
Accepted: February 4, 2015
Published: March 5, 2015

REFERENCES

Abdollahi, A., Schwager, C., Kleeff, J., Esposito, I., Domhan, S., Peschke, P., Hauser, K., Hahnfeldt, P., Hlatky, L., Debus, J., et al. (2007). Transcriptional network governing the angiogenic switch in human pancreatic cancer. Proc. Natl. Acad. Sci. USA *104*, 12890–12895.

Ahn, G.O., and Brown, J.M. (2008). Matrix metalloproteinase-9 is required for tumor vasculogenesis but not for angiogenesis: role of bone marrow-derived myelomonocytic cells. Cancer Cell *13*, 193–205.

Bility, M.T., Thompson, J.T., McKee, R.H., David, R.M., Butala, J.H., Vanden Heuvel, J.P., and Peters, J.M. (2004). Activation of mouse and human peroxisome proliferator-activated receptors (PPARs) by phthalate monoesters. Toxicol. Sci. *82*, 170–182.

Biswas, S.K., and Mantovani, A. (2010). Macrophage plasticity and interaction with lymphocyte subsets: cancer as a paradigm. Nat. Immunol. *11*, 889–896.

Brunelli, L., Cieslik, K.A., Alcorn, J.L., Vatta, M., and Baldini, A. (2007). Peroxisome proliferator-activated receptor-delta upregulates 14-3-3 epsilon in human endothelial cells via CCAAT/enhancer binding protein-beta. Circ. Res. *100*, e59–e71.

Chakravarthy, M.V., Lodhi, I.J., Yin, L., Malapaka, R.R., Xu, H.E., Turk, J., and Semenkovich, C.F. (2009). Identification of a physiologically relevant endogenous ligand for PPARalpha in liver. Cell *138*, 476–488.

Chawla, A., Lee, C.H., Barak, Y., He, W., Rosenfeld, J., Liao, D., Han, J., Kang, H., and Evans, R.M. (2003). PPARdelta is a very low-density lipoprotein sensor in macrophages. Proc. Natl. Acad. Sci. USA *100*, 1268–1273.

Condeelis, J., and Pollard, J.W. (2006). Macrophages: obligate partners for tumor cell migration, invasion, and metastasis. Cell *124*, 263–266.

Dace, D.S., Khan, A.A., Kelly, J., and Apte, R.S. (2008). Interleukin-10 promotes pathological angiogenesis by regulating macrophage response to hypoxia during development. PLoS ONE *3*, e3381.

Fan, Y., Wang, Y., Tang, Z., Zhang, H., Qin, X., Zhu, Y., Guan, Y., Wang, X., Staels, B., Chien, S., and Wang, N. (2008). Suppression of pro-inflammatory adhesion molecules by PPAR-delta in human vascular endothelial cells. Arterioscler. Thromb. Vasc. Biol. *28*, 315–321.

Fleetwood, A.J., Lawrence, T., Hamilton, J.A., and Cook, A.D. (2007). Granulocyte-macrophage colony-stimulating factor (CSF) and macrophage CSF-dependent macrophage phenotypes display differences in cytokine profiles and transcription factor activities: implications for CSF blockade in inflammation. J. Immunol. *178*, 5245–5252.

Forman, B.M., Chen, J., and Evans, R.M. (1997). Hypolipidemic drugs, polyunsaturated fatty acids, and eicosanoids are ligands for peroxisome proliferator-activated receptors alpha and delta. Proc. Natl. Acad. Sci. USA *94*, 4312–4317.

Galdiero, M.R., Garlanda, C., Jaillon, S., Marone, G., and Mantovani, A. (2013). Tumor associated macrophages and neutrophils in tumor progression. J. Cell. Physiol. *228*, 1404–1412.

Ghosh, M., Wang, H., Ai, Y., Romeo, E., Luyendyk, J.P., Peters, J.M., Mackman, N., Dey, S.K., and Hla, T. (2007). COX-2 suppresses tissue factor expression via endocannabinoid-directed PPARdelta activation. J. Exp. Med. *204*, 2053–2061.

Guignet, E.G., and Meyer, T. (2008). Suspended-drop electroporation for high-throughput delivery of biomolecules into cells. Nat. Methods *5*, 393–395.

Gupta, R.A., Tan, J., Krause, W.F., Geraci, M.W., Willson, T.M., Dey, S.K., and DuBois, R.N. (2000). Prostacyclin-mediated activation of peroxisome proliferator-activated receptor delta in colorectal cancer. Proc. Natl. Acad. Sci. USA *97*, 13275–13280.

Gupta, R.A., Wang, D., Katkuri, S., Wang, H., Dey, S.K., and DuBois, R.N. (2004). Activation of nuclear hormone receptor peroxisome proliferator-activated receptor-delta accelerates intestinal adenoma growth. Nat. Med. *10*, 245–247.

Hagemann, T., Lawrence, T., McNeish, I., Charles, K.A., Kulbe, H., Thompson, R.G., Robinson, S.C., and Balkwill, F.R. (2008). "Re-educating" tumor-associated macrophages by targeting NF-kappaB. J. Exp. Med. *205*, 1261–1268.

Han, J.K., Lee, H.S., Yang, H.M., Hur, J., Jun, S.I., Kim, J.Y., Cho, C.H., Koh, G.Y., Peters, J.M., Park, K.W., et al. (2008). Peroxisome proliferator-activated receptor-delta agonist enhances vasculogenesis by regulating endothelial progenitor cells through genomic and nongenomic activations of the phosphatidylinositol 3-kinase/Akt pathway. Circulation *118*, 1021–1033.

Hur, J., Yang, H.-M., Yoon, C.-H., Lee, C.-S., Park, K.-W., Kim, J.-H., Kim, T.-Y., Kim, J.-Y., Kang, H.-J., Chae, I.-H., et al. (2007). Identification of a novel role of T cells in postnatal vasculogenesis: characterization of endothelial progenitor cell colonies. Circulation *116*, 1671–1682.

Kang, K., Reilly, S.M., Karabacak, V., Gangl, M.R., Fitzgerald, K., Hatano, B., and Lee, C.H. (2008). Adipocyte-derived Th2 cytokines and myeloid PPARdelta regulate macrophage polarization and insulin sensitivity. Cell Metab. *7*, 485–495.

Karin, M., Lawrence, T., and Nizet, V. (2006). Innate immunity gone awry: linking microbial infections to chronic inflammation and cancer. Cell *124*, 823–835.

Kim, S., Takahashi, H., Lin, W.W., Descargues, P., Grivennikov, S., Kim, Y., Luo, J.L., and Karin, M. (2009). Carcinoma-produced factors activate myeloid cells through TLR2 to stimulate metastasis. Nature *457*, 102–106.

Kinjyo, I., Inoue, H., Hamano, S., Fukuyama, S., Yoshimura, T., Koga, K., Takaki, H., Himeno, K., Takaesu, G., Kobayashi, T., and Yoshimura, A. (2006). Loss of SOCS3 in T helper cells resulted in reduced immune responses and hyperproduction of interleukin 10 and transforming growth factor-beta 1. J. Exp. Med. *203*, 1021–1031.

Krey, G., Braissant, O., L'Horset, F., Kalkhoven, E., Perroud, M., Parker, M.G., and Wahli, W. (1997). Fatty acids, eicosanoids, and hypolipidemic agents identified as ligands of peroxisome proliferator-activated receptors by coactivator-dependent receptor ligand assay. Mol. Endocrinol. *11*, 779–791.

Kuang, D.M., Zhao, Q., Peng, C., Xu, J., Zhang, J.P., Wu, C., and Zheng, L. (2009). Activated monocytes in peritumoral stroma of hepatocellular carcinoma foster immune privilege and disease progression through PD-L1. J. Exp. Med. *206*, 1327–1337.

Kujawski, M., Kortylewski, M., Lee, H., Herrmann, A., Kay, H., and Yu, H. (2008). Stat3 mediates myeloid cell-dependent tumor angiogenesis in mice. J. Clin. Invest. *118*, 3367–3377.

Lacey, D.C., Achuthan, A., Fleetwood, A.J., Dinh, H., Roiniotis, J., Scholz, G.M., Chang, M.W., Beckman, S.K., Cook, A.D., and Hamilton, J.A. (2012). Defining GM-CSF- and macrophage-CSF-dependent macrophage responses by in vitro models. J. Immunol. *188*, 5752–5765.

Lee, C.H., Chawla, A., Urbiztondo, N., Liao, D., Boisvert, W.A., Evans, R.M., and Curtiss, L.K. (2003). Transcriptional repression of atherogenic inflammation: modulation by PPARdelta. Science *302*, 453–457.

Lee, C.S., Kwon, Y.W., Yang, H.M., Kim, S.H., Kim, T.Y., Hur, J., Park, K.W., Cho, H.J., Kang, H.J., Park, Y.B., and Kim, H.S. (2009). New mechanism of rosiglitazone to reduce neointimal hyperplasia: activation of glycogen synthase kinase-3beta followed by inhibition of MMP-9. Arterioscler. Thromb. Vasc. Biol. *29*, 472–479.

Lin, E.Y., Nguyen, A.V., Russell, R.G., and Pollard, J.W. (2001). Colony-stimulating factor 1 promotes progression of mammary tumors to malignancy. J. Exp. Med. *193*, 727–740.

Lin, E.Y., Li, J.F., Gnatovskiy, L., Deng, Y., Zhu, L., Grzesik, D.A., Qian, H., Xue, X.N., and Pollard, J.W. (2006). Macrophages regulate the angiogenic switch in a mouse model of breast cancer. Cancer Res. *66*, 11238–11246.

Liou, J.Y., Lee, S., Ghelani, D., Matijevic-Aleksic, N., and Wu, K.K. (2006). Protection of endothelial survival by peroxisome proliferator-activated receptor-delta mediated 14-3-3 upregulation. Arterioscler. Thromb. Vasc. Biol. *26*, 1481–1487.

Mantovani, A., and Locati, M. (2009). Orchestration of macrophage polarization. Blood *114*, 3135–3136.

Mantovani, A., Sozzani, S., Locati, M., Allavena, P., and Sica, A. (2002). Macrophage polarization: tumor-associated macrophages as a paradigm for polarized M2 mononuclear phagocytes. Trends Immunol. *23*, 549–555.

Mantovani, A., Allavena, P., Sica, A., and Balkwill, F. (2008). Cancer-related inflammation. Nature *454*, 436–444.

Menendez, J.A., and Lupu, R. (2007). Fatty acid synthase and the lipogenic phenotype in cancer pathogenesis. Nat. Rev. Cancer *7*, 763–777.

Mocellin, S., Panelli, M.C., Wang, E., Nagorsen, D., and Marincola, F.M. (2003). The dual role of IL-10. Trends Immunol. *24*, 36–43.

Mouchemore, K.A., and Pixley, F.J. (2012). CSF-1 signaling in macrophages: pleiotrophy through phosphotyrosine-based signaling pathways. Crit. Rev. Clin. Lab. Sci. *49*, 49–61.

Mukundan, L., Odegaard, J.I., Morel, C.R., Heredia, J.E., Mwangi, J.W., Ricardo-Gonzalez, R.R., Goh, Y.P., Eagle, A.R., Dunn, S.E., Awakuni, J.U., et al. (2009). PPAR-delta senses and orchestrates clearance of apoptotic cells to promote tolerance. Nat. Med. *15*, 1266–1272.

Müller-Brüsselbach, S., Kömhoff, M., Rieck, M., Meissner, W., Kaddatz, K., Adamkiewicz, J., Keil, B., Klose, K.J., Moll, R., Burdick, A.D., et al. (2007). Deregulation of tumor angiogenesis and blockade of tumor growth in PPAR-beta-deficient mice. EMBO J. *26*, 3686–3698.

Murdoch, C., Muthana, M., Coffelt, S.B., and Lewis, C.E. (2008). The role of myeloid cells in the promotion of tumour angiogenesis. Nat. Rev. Cancer *8*, 618–631.

Odegaard, J.I., Ricardo-Gonzalez, R.R., Red Eagle, A., Vats, D., Morel, C.R., Goforth, M.H., Subramanian, V., Mukundan, L., Ferrante, A.W., and Chawla, A. (2008). Alternative M2 activation of Kupffer cells by PPARdelta ameliorates obesity-induced insulin resistance. Cell Metab. *7*, 496–507.

Pello, O.M., De Pizzol, M., Mirolo, M., Soucek, L., Zammataro, L., Amabile, A., Doni, A., Nebuloni, M., Swigart, L.B., Evan, G.I., et al. (2012). Role of c-MYC in alternative activation of human macrophages and tumor-associated macrophage biology. Blood *119*, 411–421.

Peters, J.M., and Gonzalez, F.J. (2009). Sorting out the functional role(s) of peroxisome proliferator-activated receptor-beta/delta (PPARbeta/delta) in cell proliferation and cancer. Biochim. Biophys. Acta *1796*, 230–241.

Peters, J.M., Lee, S.S., Li, W., Ward, J.M., Gavrilova, O., Everett, C., Reitman, M.L., Hudson, L.D., and Gonzalez, F.J. (2000). Growth, adipose, brain, and skin alterations resulting from targeted disruption of the mouse peroxisome proliferator-activated receptor beta(delta). Mol. Cell. Biol. *20*, 5119–5128.

Peters, J.M., Hollingshead, H.E., and Gonzalez, F.J. (2008). Role of peroxisome-proliferator-activated receptor beta/delta (PPARbeta/delta) in gastrointestinal tract function and disease. Clin. Sci. *115*, 107–127.

Piqueras, L., Reynolds, A.R., Hodivala-Dilke, K.M., Alfranca, A., Redondo, J.M., Hatae, T., Tanabe, T., Warner, T.D., and Bishop-Bailey, D. (2007). Activation of PPARbeta/delta induces endothelial cell proliferation and angiogenesis. Arterioscler. Thromb. Vasc. Biol. *27*, 63–69.

Pollard, J.W. (2004). Tumour-educated macrophages promote tumour progression and metastasis. Nat. Rev. Cancer *4*, 71–78.

Pollard, J.W. (2009). Trophic macrophages in development and disease. Nat. Rev. Immunol. *9*, 259–270.

Rubinson, D.A., Dillon, C.P., Kwiatkowski, A.V., Sievers, C., Yang, L., Kopinja, J., Rooney, D.L., Zhang, M., Ihrig, M.M., McManus, M.T., et al. (2003). A lentivirus-based system to functionally silence genes in primary mammalian cells, stem cells and transgenic mice by RNA interference. Nat. Genet. *33*, 401–406.

Saraiva, M., and O'Garra, A. (2010). The regulation of IL-10 production by immune cells. Nat. Rev. Immunol. *10*, 170–181.

Shureiqi, I., Jiang, W., Zuo, X., Wu, Y., Stimmel, J.B., Leesnitzer, L.M., Morris, J.S., Fan, H.Z., Fischer, S.M., and Lippman, S.M. (2003). The 15-lipoxygenase-1 product 13-S-hydroxyoctadecadienoic acid down-regulates PPAR-delta to induce apoptosis in colorectal cancer cells. Proc. Natl. Acad. Sci. USA *100*, 9968–9973.

Sica, A., and Mantovani, A. (2012). Macrophage plasticity and polarization: in vivo veritas. J. Clin. Invest. *122*, 787–795.

Wang, Y.C., He, F., Feng, F., Liu, X.W., Dong, G.Y., Qin, H.Y., Hu, X.B., Zheng, M.H., Liang, L., Feng, L., et al. (2010). Notch signaling determines the M1 versus M2 polarization of macrophages in antitumor immune responses. Cancer Res. *70*, 4840–4849.

Weischenfeldt, J., and Porse, B. (2008). Bone marrow-derived macrophages (BMM): isolation and applications. CSH Protoc. *2008*, pdb.prot5080.

Xu, H.E., Lambert, M.H., Montana, V.G., Parks, D.J., Blanchard, S.G., Brown, P.J., Sternbach, D.D., Lehmann, J.M., Wisely, G.B., Willson, T.M., et al. (1999). Molecular recognition of fatty acids by peroxisome proliferator-activated receptors. Mol. Cell *3*, 397–403.

Yoon, C.H., Hur, J., Park, K.W., Kim, J.H., Lee, C.S., Oh, I.Y., Kim, T.Y., Cho, H.J., Kang, H.J., Chae, I.H., et al. (2005). Synergistic neovascularization by mixed transplantation of early endothelial progenitor cells and late outgrowth endothelial cells: the role of angiogenic cytokines and matrix metalloproteinases. Circulation *112*, 1618–1627.

Yu, K., Bayona, W., Kallen, C.B., Harding, H.P., Ravera, C.P., McMahon, G., Brown, M., and Lazar, M.A. (1995). Differential activation of peroxisome proliferator-activated receptors by eicosanoids. J. Biol. Chem. *270*, 23975–23983.

Zeng, L., O'Connor, C., Zhang, J., Kaplan, A.M., and Cohen, D.A. (2010). IL-10 promotes resistance to apoptosis and metastatic potential in lung tumor cell lines. Cytokine *49*, 294–302.

Zuo, X., Peng, Z., Moussalli, M.J., Morris, J.S., Broaddus, R.R., Fischer, S.M., and Shureiqi, I. (2009). Targeted genetic disruption of peroxisome proliferator-activated receptor-delta and colonic tumorigenesis. J. Natl. Cancer Inst. *101*, 762–767.